Chinese Chemical Letters 36 (2025) 109928

Contents lists available at ScienceDirect

Chinese Chemical Letters

journal homepage: www.elsevier.com/locate/cclet

High-temperature calcination dramatically promotes the activity of Cs/Co/Ce-Sn catalyst for soot oxidation

Meng Wang[a,b], Yan Zhang[a,b,*], Yunbo Yu[a,c,d], Wenpo Shan[a,b,*], Hong He[a,c,d]

[a] Center for Excellence in Regional Atmospheric Environment, Institute of Urban Environment, Chinese Academy of Sciences, Xiamen 361021, China
[b] Zhejiang Key Laboratory of Urban Environmental Processes and Pollution Control, Ningbo Urban Environment Observation and Research Station, Institute of Urban Environment, Chinese Academy of Sciences, Ningbo 315800, China
[c] State Key Joint Laboratory of Environment Simulation and Pollution Control, Research Center for Eco-Environmental Sciences, Chinese Academy of Sciences, Beijing 100085, China
[d] University of Chinese Academy of Sciences, Beijing 100049, China

ARTICLE INFO

Article history:
Received 24 November 2023
Revised 24 March 2024
Accepted 25 April 2024
Available online 25 April 2024

Keywords:
Soot oxidation
Calcination
Surface defects
Surface-active oxygen species
NO_2

ABSTRACT

Catalytic oxidation of soot is of great importance for emission control on diesel vehicles. In this work, a highly active Cs/Co/Ce-Sn catalyst was investigated for soot oxidation, and it was unexpectedly found that high-temperature calcination greatly improved the activity of the catalyst. When the calcination temperature was increased from 500 °C to 750 °C, T_{50} decreased from 456.9 °C to 389.8 °C in a $NO/O_2/H_2O/N_2$ atmosphere. Characterization results revealed that high-temperature calcination can promote the ability to transfer negative charge density from Cs to other metal cations in Cs/Co/Ce-Sn, which will facilitate the production of more oxygen defects and the generation of more surface-active oxygen species. Surface-active oxygen species are beneficial to the oxidation of NO to NO_2, leading to the high yield of NO_2 exploitation. Therefore, the Cs/Co/Ce-Sn catalyst calcined at 750 °C demonstrated higher activity than that calcined at 500 °C. This work provides a pathway to prepare high efficiency catalysts for the removal of soot and significant insight into the effects of calcination on soot oxidation catalysts.

Soot particulate released from diesel engines exhaust is one of the major sources of particulate matter emission, which not only cause pollution of the atmospheric environment, but also seriously endanger the human respiratory system [1–3]. The coupling of DPF (diesel particulate filter) and soot oxidation catalysts, has been regarded as an effective technique to control soot emission from diesel vehicles [4,5]. The key problem is how to develop high-performance soot oxidation catalysts.

To date, a series of high-efficiency catalysts for soot oxidation have been reported, including noble metal-based catalysts [6,7], rare earth oxides [8], transition metal oxides [9,10] and other mixed metal oxides [11,12]. It is widely acknowledged that the noble metal-containing catalysts are still the main commercial catalysts for soot oxidation. Yet, the reserves of noble metals are limited, and the cost is getting higher and higher [13,14]. Therefore, it is urgent to develop high-efficiency non-noble metal-based catalysts for soot purification. Ceria-based catalysts present great promise as soot oxidation catalysts, due to their oxygen storage and release ability [15]. For instance, Chen *et al.* found that with respect to pure soot, the T_{50} of a CeO_2 nanorod catalyst decreased from 517 °C to 415 °C under tight contact [16]. Thus, Ce-based oxide catalysts presented good potentiality on the application of diesel soot combustion.

Various strategies for improving soot oxidation performance of Ce-based oxide catalysts have been reported, such as doping with transition metals or using supported transition metal oxides [8,17,18], adding alkali or alkali earth metals [19,20], fabricating special morphologies [21,22]. Sn was doped into cerium oxide to improve oxygen storage capacity (OSC) of CeO_2, because the reversible $Sn^{4+} \leftrightarrow Sn^{2+}$ redox process involves two electron transfer. In particular, doping with alkali metals is widely used, due to their excellent electron donation properties or high mobility. For example, in Ura's work, addition of potassium showed great positive effects on the soot oxidation activity of the $SrTiO_3$ catalyst, lowering the soot ignition temperature by 100 °C [23]. Wang *et al.* also found that the addition of alkali metal oxides in SnO_2 catalysts can promote the generation of more abundant and mobile oxygen species, which would be good for soot oxidation [24]. Zhang *et al.* found that doping with Cs can enhance the catalytic performance of CeO_2 catalysts for soot oxidation more than the more commonly studied K, due to the easier electron donation from Cs_2O species

* Corresponding authors.
E-mail addresses: yzhang3@iue.ac.cn (Y. Zhang), wpshan@iue.ac.cn (W. Shan).

https://doi.org/10.1016/j.cclet.2024.109928
1001-8417/

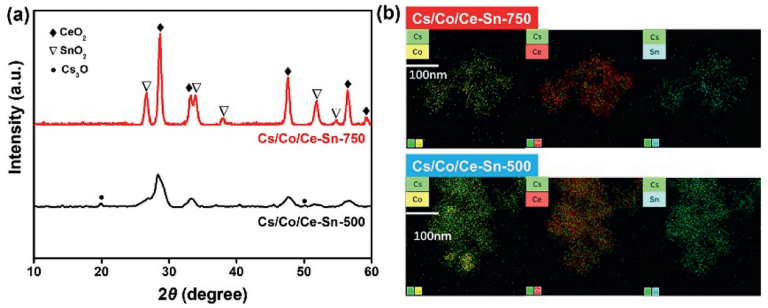

Fig. 1. (a) XRD patterns and (b) Element mapping results from EDX of the as-prepared catalysts.

[25]. In addition, it has been reported that the calcination temperature can significantly influence the performance of catalysts containing alkali metals, and that high-temperature calcination may induce deactivation. For instance, Neyertz *et al.* revealed that a K/Ce-based catalyst was deactivated after calcination at 800 °C for 24 h, with the T_{50} increasing from 448 °C to 545 °C [26]. Similarly, An *et al.* also found that potassium-containing catalysts were deactivated after undergoing repeated thermal aging cycles [27].

In our previous study, we developed a Cs/Co/Ce-Sn (10%Cs/3%Co/Ce-Sn) catalyst with excellent soot oxidation activity, due to the dual positive effects of Cs [28]. In this work, the effect of calcination temperature on the Cs/Co/Ce-Sn catalyst was investigated by calcining the catalyst at low temperature (500 °C) and high temperature (750 °C), respectively. Unexpectedly, the Cs/Co/Ce-Sn catalyst calcined at 750 °C exhibited much higher activity for soot oxidation than that calcined at 500 °C. The reason for the promotional effect of high-temperature calcination was investigated and elucidated via various characterization methods.

X-ray diffraction (XRD) measurements were utilized to analyze the crystal structures of the Cs/Co/Ce-Sn-500 and Cs/Co/Ce-Sn-750 catalysts. As shown in Fig. 1a, the typical peaks of CeO_2 were mainly observed in all the catalysts (PDF #43–1002). For the Cs/Co/Ce-Sn-500 catalyst, besides the major diffraction peaks of CeO_2, two minor diffraction peaks of Cs oxide (PDF #09–0111) at around 20° and 50° were also detected. After high-temperature calcination (750 °C), some diffraction peaks for SnO_2 were formed (PDF #41–1445). However, no peaks associated with Cs or Co oxides were observed, which could be due to the high dispersion of Cs and Co oxides. The elemental mapping of the Cs/Co/Ce-Sn-500 and Cs/Co/Ce-Sn-750 catalysts was carried out (Fig. 1b) to confirm the high dispersion of Cs and Co oxides. Clearly, the Cs and Co oxides for Cs/Co/Ce-Sn-750 catalyst were well dispersed, which agreed with the XRD results.

X-ray photoelectron spectrometry (XPS) measurements were employed to study the effect of calcination temperature on the states of Cs species in the catalyst. As shown in Fig. 2a, two typical peaks relating to Cs^+ cations were observed for the Cs/Co/Ce-Sn catalysts [19]. Notably, the Cs 3d peaks of Cs/Co/Ce-Sn-750 (724.6, 738.5 eV) exhibited a clear shift to higher energy in comparison with Cs/Co/Ce-Sn-500 (724.0, 737.9 eV). This result could arise because high-temperature calcination induced the Cs^+ to transfer more negative charge density to oxide anions and subsequently affected the Co, Ce and Sn metal cations [25,29].

XPS and X-ray absorption fine structure (XAFS) technologies were applied to study the surface properties of Co species in the Cs/Co/Ce-Sn-500 and Cs/Co/Ce-Sn-750 catalysts. The XPS spectra of Co 2p for the catalysts were deconvoluted to reveal four peaks, the peaks located at 781.4 and 796.3 eV could be attributed to Co^{2+}, and the others assigned to Co^{3+} for the Cs/Co/Ce-Sn-500 catalyst [2]. As the calcination temperature increasing from 500 °C to 750 °C, the binding energy of Co species decreased about 0.5 eV, indicating that more electrons from the Cs dopant were shifted towards the Co species. Thus, the ratio of Co^{2+}/Co^{3+} for the Cs/Co/Ce-Sn-750 sample increased from 1.14 to 1.32 (Fig. 2b). Each Co^{2+} ion is related to a neighboring oxygen defect, which can easily activate the gaseous oxygen to generate active oxygen species [30]. To further explore the influence of calcination temperature on the state of Co species, XAFS measurements were used. Fig. 2c shows that the Co K-edge XAFS spectra of the Cs/Co/Ce-Sn-500 and Cs/Co/Ce-Sn-750 catalysts were similar as that of Co_3O_4. As shown in Fig. 2d, there are three peaks located at 1.92, 2.89 and 3.39 Å in the R-space spectra of the Co-K edge, which are related to the first Co-O, the first Co-Co_1 and the second Co-Co_2 shells, respectively [31]. For the Cs/Co/Ce-Sn-750 sample, it performed a relatively smaller coordination number for the Co-O shell than the Cs/Co/Ce-Sn-500 sample (Table S1 in Supporting information), which suggested that high-temperature calcination promotes the generation of oxygen defects.

The XPS spectra of Ce 3d for the Cs/Co/Ce-Sn-500 and Cs/Co/Ce-Sn-750 catalysts can be deconvoluted into the ten characteristic peaks (Fig. S1a in Supporting information). The v, v_2, v_3, u, u_2 and u_3 were attributed to the Ce^{4+} species, and the others were related to reduced cerium species Ce^{3+} [32]. It was clearly found that the Ce^{3+}/Ce^{4+} ratio for the Cs/Co/Ce-Sn catalyst increased from 0.41 to 0.50 with the increase in the calcination temperature from 500 °C to 750 °C. This result suggested that high-temperature calcination is beneficial to the formation of Ce^{3+}. In addition, the Ce L_{III} XANES results revealed that in comparison with Cs/Co/Ce-Sn-500, the ratio of Ce^{3+}/Ce^{4+} for Cs/Co/Ce-Sn-750 increased from 29.8% to 39.3% (Fig. S2 in Supporting information). The higher ratio of Ce^{3+}/Ce^{4+} in the catalyst, the more oxygen defects would be produced, which is beneficial for soot oxidation.

The Sn species in the catalysts were explored by XPS, and the results are exhibited in Fig. S1b (Supporting information). It was noteworthy that with the increase in the calcination temperature from 500 °C to 750 °C, the ratio of surface Sn^{2+}/Sn^{4+} of Cs/Co/Ce-Sn increased from 1.06 to 1.29, indicating the formation of more surface defects.

Two peaks were identified in the O 1s XPS profiles of the Cs/Co/Ce-Sn-500 and Cs/Co/Ce-Sn-750 catalysts. The peak of the surface-adsorbed oxygen species (O_α) was located at 531–532.1 eV, and the peak centered at lower binding energy of 528.9–530.5 eV was assigned to lattice oxygen species (O_β) [22,33]. As shown in Fig. 2e, when the calcination temperature of the Cs/Co/Ce-Sn sample was increased from 500 °C to 750 °C, it was clearly found that the ratio of O_α/O_β increased from 0.40 to 0.58. This indicated that the high-temperature calcination induced the production of more abundant oxygen defects, and these defects would be beneficial to activating gas oxygen to generate active oxygen species.

Electron paramagnetic resonance (EPR) was carried out to further analyze the oxygen defects of the Cs/Co/Ce-Sn-500 and Cs/Co/Ce-Sn-750 catalysts. The spectrum in Fig. 2f exhibits a

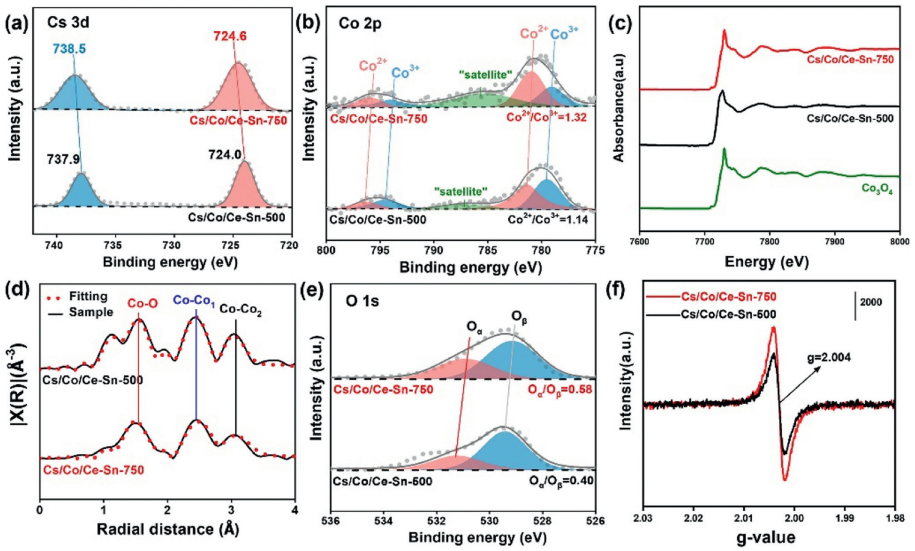

Fig. 2. XPS results of (a) Cs 3d, (b) Co 2p of the Cs/Co/Ce-Sn samples. (c) The normalized XANES spectra of Co K-edge, (d) EXAFS spectra at Co K-edge of the Cs/Co/Ce-Sn-750 and Cs/Co/Ce-Sn-500 catalysts. (e) XPS results of O 1s of the Cs/Co/Ce-Sn samples, and (f) EPR profiles of the Cs/Co/Ce-Sn-750 and Cs/Co/Ce-Sn-500 catalysts.

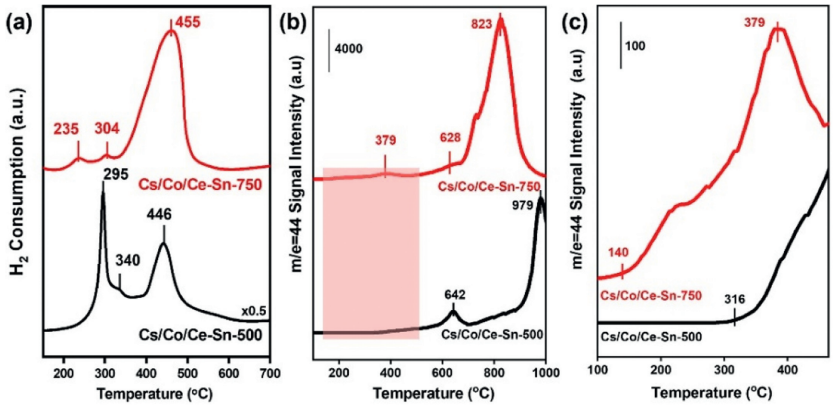

Fig. 3. (a) H_2-TPR, (b) soot-TPR, and (c) enlarged soot-TPR curves of the Cs/Co/Ce-Sn-750 and Cs/Co/Ce-Sn-500 catalysts.

symmetrical EPR signal at $g = 2.004$, uncovering the existence of oxygen defects in both catalysts [34,35]. The oxygen vacancy concentration is related to EPR signal intensity. The stronger EPR signal intensity is, the more oxygen vacancies would be presented. Interestingly, Cs/Co/Ce-Sn-750 exhibited a much stronger signal than the Cs/Co/Ce-Sn-500 catalyst, which suggested that it contained more oxygen defects. This result is consistent with the XPS and XAFS results.

To evaluate the influence of calcination temperature on the redox properties, H_2-TPR tests were performed. As shown in Fig. 3a, the H_2-TPR curves of Cs/Co/Ce-Sn-500 includes three peaks at 295 °C, 340 °C, and 446 °C, respectively. The reduction peaks located at 295 °C and 340 °C can be attributed to the reduction of Co^{3+} to Co^{2+} and then to Co, respectively [21,36]. The last reduction peak centered at 446 °C is related to the reduction of Ce^{4+} to Ce^{3+} in 425–665 °C [37,38] and Sn^{4+} to Sn^{2+} or Sn in 400–675 °C [21,24,39]. Interestingly, when the calcination temperature increased to 750 °C, the reduction peaks of Co species moved towards lower temperatures, which covered that the high-temperature calcination had an active impact on the redox ability of Cs/Co/Ce-Sn.

O_2-TPD was applied to explore the influence of calcination temperature on the ability to activate oxygen species. As shown in Fig. S3 (Supporting information), for the Cs/Co/Ce-Sn-500 sample, the staring desorption temperature of active oxygen species was 359 °C. Interestingly, when the calcination temperature was promoted from 500 °C to 750 °C, the starting desorption temperature of active oxygen species decreased to 346 °C for Cs/Co/Ce-Sn-750, which suggested that the mobility of active oxygen species for Cs/Co/Ce-Sn-750 was improved, corresponding to the H_2-TPR result. The soot-TPR result also confirmed that high-temperature calcination could increase the mobility of active oxygen species for the Cs/Co/Ce-Sn catalyst (Figs. 3b and c). In addition, DMPO-trapped ESR experiments were also conducted to test the reactive oxygen species. As shown in Fig. S4 (Supporting information), characteristic peaks of O_2^- species were captured, and Cs/Co/Ce-Sn-750 exhibited a much stronger signal than the Cs/Co/Ce-Sn-500 catalyst, indicating that high-temperature calcination can promote the production of more reactive oxygen species [40–42]. Above all, the high-temperature calcination at 750 °C for Cs/Co/Ce-Sn was beneficial to the activating ability of chemisorbed oxygen.

The activity of the Cs/Co/Ce-Sn catalyst calcined at 500 °C and 750 °C for soot catalytic oxidation was investigated by the soot-TPO method under loose contact. The soot conversion levels of the Cs/Co/Ce-Sn-500 and Cs/Co/Ce-Sn-750 catalysts are shown in Fig. S6 (Supporting information) and Fig. 4a. When soot was mixed with the Cs/Co/Ce-Sn-500 catalyst, the T_{50} was 467.5 °C under an $O_2/H_2O/N_2$ atmosphere. Yet, as the increase of the calcination temperature to 750 °C, it was surprisingly found that the T_{50} was

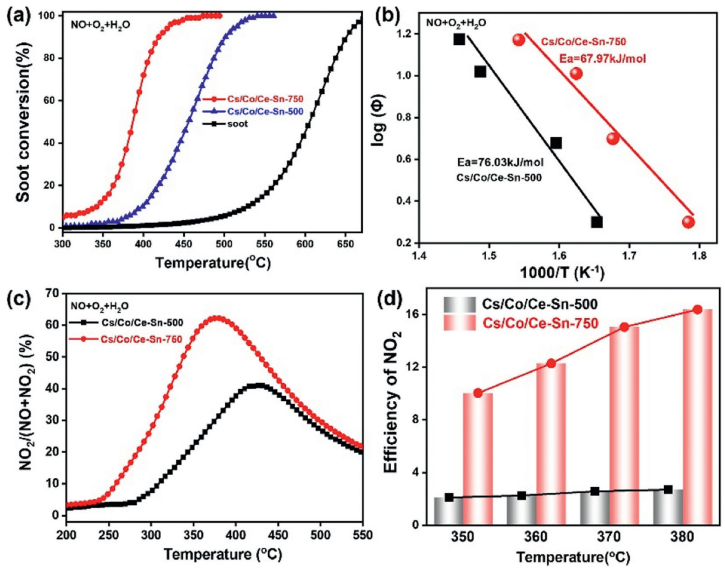

Fig. 4. (a) Soot conversion, (b) Ozawa plots for soot conversion of the as-prepared samples with different heating rates (2, 5, 10, and 15 °C/min), under loose contact mode and a GHSV of 300,000 mL g^{-1} h^{-1}. (c) $NO_2/(NO+NO_2)$ ratio in the outlet feed over the as-prepared catalysts in NO-TPO test without soot. (d) Utilization efficiency of NO_2 at different temperatures over the catalysts. Feed composition: 1000 ppm NO, 5% H_2O, 10% O_2, and N_2 balance.

lowered to 446 °C (Fig. S6), indicating that the high-temperature calcination has a certain promotion effect for soot oxidation. The activities of soot oxidation for the Cs/Co/Ce-Sn catalyst calcined at 500 °C and 750 °C in $NO/O_2/H_2O/N_2$ atmosphere are shown in Fig. 4a. When NO was added into the reaction atmosphere, all the catalysts performed enhanced catalytic performance. For instance, the T_{50} values of the Cs/Co/Ce-Sn-500 and Cs/Co/Ce-Sn-750 catalysts decreased to 456.9 and 389.8 °C, respectively, and the CO_2 selectivity for both catalysts was close to 100% (Fig. S7 in Supporting information). Fig. S8 (Supporting information) revealed that the addition of H_2O was beneficial to soot oxidation, which could be due to the wettability of water vapor increases the contact efficiency between the catalysts and soot particles. The five consecutive cycles test was used to study the stability of the Cs/Co/Ce-Sn-750 catalyst during in $NO/O_2/H_2O/N_2$ atmosphere (Fig. S9 in Supporting information), and the result indicated that the Cs/Co/Ce-Sn-750 catalyst was stable for soot catalytic combustion. Additionally, the soot oxidation performance was also evaluated in different heating rates. As shown in Fig. S10 (Supporting information), the Cs/Co/Ce-Sn-750 catalyst still exhibited better catalytic activity than Cs/Co/Ce-Sn-500 catalyst, even in the heating rates of 5 °C/min or 2 °C/min. Table S2 (Supporting information) listed the T_{50} of the Cs/Co/Ce-Sn-750 and some catalysts reported in previous literatures [6,43-46]. Obviously, the Cs/Co/Ce-Sn-750 catalyst had lower T_{50} value, indicating that a cheap and high-performance catalyst for soot catalytic oxidation was developed.

To study the intrinsic activities of the Cs/Co/Ce-Sn-500 and Cs/Co/Ce-Sn-750 catalysts, the activation energy was calculated for soot oxidation using different catalysts at the same soot conversion level *via* the Ozawa method [2,22]. As shown in Fig. 4b, the apparent activation energy of the Cs/Co/Ce-Sn-500 sample was 76.03 kJ/mol. Remarkably, as the calcination temperature was increased to 750 °C, the apparent activation energy was decreased to 67.97 kJ/mol, indicating that calcinating at high temperature could significantly reduce the energy barrier.

The NO-TPO test was also carried out to further study the influence of NO on soot catalytic combustion, and the results are performed in Fig. 4c. The NO to NO_2 conversion curves of the Cs/Co/Ce-Sn-500 and Cs/Co/Ce-Sn-750 catalysts both showed a volcano trend. As shown in Fig. 4c, the NO oxidation activity of Cs/Co/Ce-Sn-750 at low temperature was clearly higher than that of Cs/Co/Ce-Sn-500 in $NO/O_2/H_2O/N_2$ atmosphere, which revealed that the high-temperature calcination had a positive effect on the NO oxidation activity. Under this condition, the maximum conversion of NO reached 62.2% at 380.4 °C over the Cs/Co/Ce-Sn-750 catalyst. To further reveal the effect of NO_2 on soot oxidation, the NO_2 utilization efficiencies for Cs/Co/Ce-Sn-500 and Cs/Co/Ce-Sn-750 catalysts were calculated *via* Eq. S1 (Supporting information) at different temperatures, and the results are shown in Fig. 4d. Interestingly, the NO_2 utilization efficiency of Cs/Co/Ce-Sn-750 is much higher than that of Cs/Co/Ce-Sn-500, indicating that high-temperature calcination is beneficial to the NO_2 utilization efficiency.

Figs. S11 and S12 (Supporting information) show the EPR, Cs 3d XPS, Co 2p, Ce 3d, Sn 3d, and O 1s XPS profiles of the Cs/Co/Ce-Sn-750 sample before and after five soot-TPO cycles in a $O_2/NO/H_2O/N_2$ atmosphere. The Cs 3d, Co 2p, Ce 3d, Sn 3d, and O 1s XPS profiles for the spent Cs/Co/Ce-Sn-750 catalyst were alike to those of the fresh Cs/Co/Ce-Sn-750 catalyst, suggesting high surface chemical stability (Figs. S11a, b, c and Fig. S12). In addition, the EPR profiles exhibited similar signals for the fresh and spent Cs/Co/Ce-Sn-750 catalyst (Cs/Co/Ce-Sn-750-S), which indicated that the oxygen defects in the Cs/Co/Ce-Sn-750 catalyst were stable (Fig. S11d). All the results demonstrated that the Cs/Co/Ce-Sn catalyst calcined at high temperature (750 °C) was stable for soot oxidation.

In this study, it was found that with the increase in calcination temperature from 500 °C to 750 °C, T_{50} of the 10%Cs/3%Co/Ce-Sn catalyst decreased from 456.9 °C to 389.8 °C in a $NO/O_2/H_2O/N_2$ atmosphere (Fig. 4a), which indicated that high-temperature calcination at 750 °C was beneficial to the soot oxidation performance. The characterization results showed that high-temperature calcination could drive the Cs to transfer more negative charge density to the Co, Ce and Sn metal cations in the Cs/Co/Ce-Sn sample, which induced the production of more oxygen defects (Fig. 2a). The XPS, XAFS, and EPR results (Figs. 2b-f, Figs. S1 and S2) indicated that Cs/Co/Ce-Sn-750 had more surface oxygen defects than Cs/Co/Ce-Sn-500. The O 1s XPS, O_2-TPD, Soot-TPR and DMPO-trapped EPR (Fig. 3, Figs. S3 and S4) results further revealed that high-temperature calcination can facilitate the production of more surface-active oxygen for the Cs/Co/Ce-Sn sample, due to the

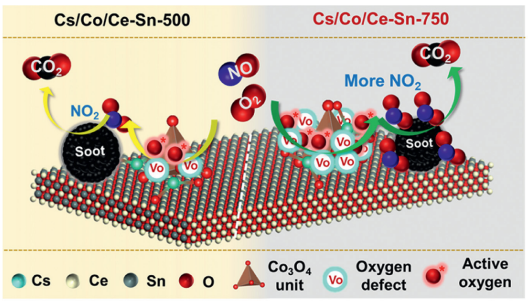

Fig. 5. Schematic diagram of soot catalytic oxidation process of the Cs/Co/Ce-Sn-500 and Cs/Co/Ce-Sn-750 catalysts.

generation of more oxygen defects. In addition, the results of NO-TPO and NO_2 utilization efficiency tests (Figs. 4c and d) proved that high-temperature calcination had a promotional effect on driving NO_2 to take part in soot oxidation, which is associated with the formation of more surface-active oxygen species. Based on the above discussion, Fig. 5 shows the influence of calcination temperature on the soot oxidation activity of Cs/Co/Ce-Sn. The high-temperature calcination of the Cs/Co/Ce-Sn sample is good for the formation of more oxygen defects, *via* the transfer of more negative charge density from Cs to other metal cations. The generated oxygen defects then facilitate the activation of surface chemisorbed oxygen, and the formed active oxygen species can take part in soot oxidation and further oxidize NO to NO_2 to accelerate soot combustion. Therefore, high-temperature calcination endowed the Cs/Co/Ce-Sn sample with superior soot oxidation performance.

In conclusion, this work unexpectedly found that a Cs/Co/Ce-Sn catalyst calcined at a high temperature of 750 °C showed much higher soot oxidation activity than that calcined at 500 °C. Characterization results revealed that high-temperature calcination can drive the alkali metal Cs to transfer more negative charge density to other metal cations, inducing the production of more oxygen defects on the surface of the Cs/Co/Ce-Sn sample. The increase in the number of oxygen defects had advantage in the formation of more active oxygen species, thus improving the NO_2 utilization efficiency for soot catalytic oxidation. Therefore, Cs/Co/Ce-Sn-750 performed superior soot oxidation activity. This work provides an in-depth understanding of the influence of calcination temperature on this soot oxidation catalyst and may aid in the design and synthesis of high efficiency catalysts for the removal of soot.

Declaration of competing interest

The authors declare that they have no known competing financial interests or personal relationships that could have appeared to influence the work reported in this paper.

CRediT authorship contribution statement

Meng Wang: Data curation, Formal analysis, Investigation, Writing – original draft. **Yan Zhang:** Conceptualization, Formal analysis, Funding acquisition, Supervision, Writing – review & editing. **Yunbo Yu:** Formal analysis, Validation. **Wenpo Shan:** Funding acquisition, Supervision, Writing – review & editing, Conceptualization. **Hong He:** Supervision, Writing – review & editing.

Acknowledgments

This work was supported by the National Natural Science Foundation of China (Nos. 22206183, 52225004), the National Key R&D Program of China (No. 2022YFC3701804), the Strategic Priority Research Program of the Chinese Academy of Sciences (No. XDA23010201), the Youth Innovation Promotion Association of Chinese Academy of Sciences (No. 2022309).

Supplementary materials

Supplementary material associated with this article can be found, in the online version, at doi:10.1016/j.cclet.2024.109928.

References

[1] A. Ma, L. Gu, Y. Zhu, et al., Chem. Commun. 53 (2017) 8517–8520.
[2] L. He, Y. Zhang, Y. Zang, et al., ACS Catal. 11 (2021) 14224–14236.
[3] D. Jampaiah, V.K. Velisoju, D. Devaiah, et al., Appl. Surf. Sci. 473 (2019) 209–221.
[4] L. Lizarraga, S. Souentie, A. Boreave, et al., Environ. Sci. Technol. 45 (2011) 10591–10597.
[5] K. Villani, W. Vermandel, K. Smets, et al., Environ. Sci. Technol. 40 (2006) 2727–2733.
[6] S. Liu, X. Wu, D. Weng, M. Li, J. Fan, Appl. Catal. B: Environ. 138-139 (2013) 199–211.
[7] J. Lee, D. Jo, J. Choung, et al., J. Hazard. Mater. 403 (2021) 124085.
[8] X. Lin, S. Li, H. He, et al., Appl. Catal. B: Environ. 223 (2018) 91–102.
[9] S.K. Megarajan, S. Rayalu, M. Nishibori, Y. Teraoka, N. Labhsetwar, ACS Catal, 5 (2014) 301–309.
[10] D. Mukherjee, D. Devaiah, P. Venkataswamy, et al., New J. Chem. 42 (2018) 14149–14156.
[11] W.L. Wang, Q. Meng, Y. Xue, et al., J. Catal. 366 (2018) 213–222.
[12] J. Zokoe, C. Su, P.J. McGinn, Ind. Eng. Chem. Res. 58 (2019) 11891–11901.
[13] R. Neha, R. Prasad, S.V. Singh, J. Environ. Chem. Eng. 8 (2020) 103945.
[14] P. Zhang, X. Mei, X. Zhao, et al., Environ. Sci. Technol. 55 (2021) 11245–11254.
[15] E. Aneggi, C. Leitenburg, G. Dolcetti, A. Trovarelli, Catal. Today 114 (2006) 40–47.
[16] Z. Chen, L. Chen, M. Jiang, et al., Appl. Surf. Sci. 510 (2020) 145401.
[17] M. Kang, M. Song, C. Lee, Appl. Catal. A: Gen. 251 (2003) 143–156.
[18] I. Atribak, A. Bueno-López, A. García-García, J. Catal. 259 (2008) 123–132.
[19] R. Liu, X. Feng, X. Xu, et al., Appl. Surf. Sci. 509 (2020) 145363.
[20] P. Legutko, P. Stelmachowski, X. Yu, et al., ACS Catal. 13 (2023) 3395–3418.
[21] Y. Tsai, N. Huy, J. Lee, Y. Lin, K. Lin, Chem. Eng. J. 395 (2020) 124939.
[22] B. Cui, L. Zhou, K. Li, et al., Appl. Catal. B: Environ. 267 (2020) 118670.
[23] B. Ura, J. Trawczyński, A. Kotarba, et al., Appl. Catal. B: Environ. 101 (2011) 169–175.
[24] C. Rao, J. Shen, F. Wang, et al., Appl. Surf. Sci. 435 (2018) 406–414.
[25] Q. Li, Y. Xin, Z. Zhang, X. Cao, Chem. Eng. J. 337 (2018) 654–660.
[26] C.A. Neyertz, E.D. Banús, E.E. Miró, C.A. Querini, Chem. Eng. J. 248 (2014) 394–405.
[27] H. An, P. McGinn, Appl. Catal. B: Environ. 62 (2006) 46–56.
[28] M. Wang, Y. Zhang, Y. Yu, W. Shan, H. He, Appl. Catal. B: Environ. 285 (2021) 119850.
[29] D. Sarma, C.D. Malliakas, K.S. Subrahmanyam, S.M. Islam, M.G. Kanatzidis, Chem. Sci. 7 (2016) 1121–1132.
[30] M. Zhao, J. Deng, J. Liu, et al., ACS Catal. 9 (2019) 7548–7567.
[31] J. Wang, L. Lin, Y. He, et al., Electrochim. Acta 254 (2017) 72–78.
[32] M. Kurnatowska, W. Mista, P. Mazur, L. Kepinski, Appl. Catal. B: Environ. 148-149 (2014) 123–135.
[33] G. Grzybek, P. Stelmachowski, S. Gudyka, et al., Appl. Catal. B: Environ. 180 (2016) 622–629.
[34] Y. Zheng, Y. Su, C. Pang, et al., Environ. Sci. Technol. 56 (2022) 1905–1916.
[35] Y. Zheng, K. Fu, Z. Yu, et al., J. Mater. Chem. A 10 (2022) 14171–14186.
[36] W. Shao, Z. Wang, X. Zhang, et al., Catal. Lett. 146 (2016) 1397–1407.
[37] T. Andana, M. Piumetti, S. Bensaid, et al., Appl. Catal. B: Environ. 216 (2017) 41–58.
[38] J. Lee, S. Lee, J. Choung, C. Kim, K. Lee, Appl. Catal. B: Environ. 246 (2019) 356–366.
[39] Z. Liu, X. Feng, Z. Zhou, Y. Feng, J. Li, Appl. Surf. Sci. 428 (2018) 526–533.
[40] Y. Jiang, S. Li, S. Wang, et al., J. Am. Chem. Soc. 145 (2023) 2698–2707.
[41] F. Xiao, Z. Wang, J. Fan, Angew. Chem. Int. Ed. 60 (2021) 10375–10383.
[42] R. Song, H. Chi, Q. Ma, J. Am. Chem. Soc. 143 (2021) 13664–13674.
[43] M. Sun, L. Wang, B. Feng, et al., Catal. Today 175 (2011) 100–105.
[44] D. Andana, M. Piumetti, S. Bensaid, et al., Appl. Catal. B: Environ. 209 (2017) 295–310.
[45] X. Wu, F. Lin, L. Wang, D. Weng, Z. Zhou, J. Environ. Sci. 23 (2011) 1205–1210.
[46] Y. Wei, Z. Zhao, X. Yu, Catal. Sci. Technol. 3 (2013) 2958–2970.